



OPEN ACCESS

EDITED BY

Xupeng Cao,
Chinese Academy of Sciences (CAS), China

REVIEWED BY

Ali Parsaeimehr,
Delaware State University, United States
Yenny Risjani,
University of Brawijaya, Indonesia

*CORRESPONDENCE

Joon-Woo Ahn
✉ joon@kaeri.re.kr

†These authors have contributed
equally to this work and share
first authorship

RECEIVED 04 January 2024

ACCEPTED 07 May 2024

PUBLISHED 21 May 2024

CITATION

Han S-I, Heo YM, Jeon MS, Kyung S, Kang S,
Kwon S-J, Ryu JH, Kim JH and Ahn J-W
(2024) The effect of exopolysaccharides from
EMS-induced *Porphyridium cruentum* mutant
on human epidermal and dermal layers.
Front. Mar. Sci. 11:1365311.
doi: 10.3389/fmars.2024.1365311

COPYRIGHT

© 2024 Han, Heo, Jeon, Kyung, Kang, Kwon,
Ryu, Kim and Ahn. This is an open-access
article distributed under the terms of the
[Creative Commons Attribution License \(CC BY\)](https://creativecommons.org/licenses/by/4.0/).
The use, distribution or reproduction in other
forums is permitted, provided the original
author(s) and the copyright owner(s) are
credited and that the original publication in
this journal is cited, in accordance with
accepted academic practice. No use,
distribution or reproduction is permitted
which does not comply with these terms.

The effect of exopolysaccharides from EMS-induced *Porphyridium cruentum* mutant on human epidermal and dermal layers

Sang-Il Han^{1†}, Young Mok Heo^{2†}, Min Seo Jeon¹,
Seoyeon Kyung², Seunghyun Kang², Soon-Jae Kwon¹,
Jai Hyunk Ryu¹, Jae Hoon Kim¹ and Joon-Woo Ahn^{1*}

¹Advanced Radiation Technology Institute, Korea Atomic Energy Research Institute, Jeongseup,
Republic of Korea, ²Research & Innovation Center, COSMAX BTI, Seongnam, Republic of Korea

Introduction: Microalgae biotechnology utilizes species like *Porphyridium cruentum* for their valuable phycobiliproteins and exopolysaccharides, which have potential industrial applications and health benefits, particularly in skin condition improvement.

Methods: A mutant of *P. cruentum* LIMS-PS-1061 was developed through ethyl methanesulfonate mutagenesis and subsequent colony screening to study changes in its biomass production and pigment composition under different lighting conditions.

Results and discussion: The mutant exhibited a 33.9% increase in dry weight under white light compared to the wild type. Despite maintaining the total pigment content, specific components changed significantly: chlorophyll content decreased 2.20- and 3.61-fold under white and blue light respectively, while phycobiliproteins increased 1.59- and 1.23-fold under the same conditions. These alterations suggest a compensatory mechanism for maintaining photosynthetic capacity. Furthermore, the exopolysaccharides of *P. cruentum* upregulated genes related to skin moisturization, barrier enhancement, and elasticity, and promoted wound healing through fibroblast migration. This supports the proposed mechanism of action for *P. cruentum*'s exopolysaccharides in improving human skin conditions by integrating the effects of aquaporin 3, filaggrin, involucrin, loricrin, elastin, and fibrillin-1.

KEYWORDS

Porphyridium cruentum, ethyl methanesulfonate, phycobiliproteins, exopolysaccharides, skin moisturization, elasticity, barrier enhancement, wound healing

1 Introduction

Marine microalgae are known as promising sources of high-value compounds, such as carotenoids, phycobiliproteins, polysaccharides, and polyunsaturated fatty acids (Li et al., 2019). Among them, *Porphyridium* sp., unicellular red microalgae belonging to Rhodophyta, are particularly notable for their capacity to produce large amounts of commercially valuable compounds, including sulfated polysaccharides (SPs; major components of exopolysaccharides (EPS) in *Porphyridium* sp.) and phycobiliproteins (PBs) composed of phycoerythrin (PE), phycocyanin (PC), and allophycocyanin (APC) (Han et al., 2020). PBs, characterized by their striking coloration and intense fluorescence, serve as key components of the light-harvesting antenna complexes found in cyanobacteria and certain algal groups, including Rhodophyta and Cryptomonads (Lauceri et al., 2019). From a commercial perspective, PBs have several applications, such as fluorescent markers, ingredients in cosmetics, and natural colorants in food products (Leney et al., 2018). In particular, PE exhibits the highest level of fluorescence among natural pigments because of its superior absorption coefficient and quantum yield compared to other fluorescent pigments (Isailovic et al., 2006). Also, both PC and APC are known to have potential health benefits, including antioxidant and anti-inflammatory properties (Liu et al., 2012; Ashaolu et al., 2021).

SPs synthesized by *Porphyridium* sp. are complex high-molecular-weight polymers composed primarily of sugar residue with sulfated modifications (Sun et al., 2009). The harvesting process of SPs is facilitated by their characteristic exogenous secretion, which leads to the formation of a protective matrix encapsulating the cells. This feature significantly simplifies the extraction of SPs from culture. Moreover, SPs derived from *Porphyridium* sp. exhibit a multitude of bioactivities, including antioxidant, anti-inflammatory, antiviral, anticoagulant, immunomodulatory, and skin-hydrating activities (Andrew and Jayaraman, 2021; Casas-Arrojo et al., 2021); furthermore, recent studies indicate that they stimulate the immune response to vibriosis and are non-toxic (Risjani et al., 2021). Owing to the efficient extraction methods and the diverse bioactive properties, SPs from *Porphyridium* sp. have garnered interest from various industrial fields, notably the pharmaceutical and cosmetic industries.

Despite the several benefits presented, the strategic development of economically viable strains is essential to advance the current state of the microalgae industry. The development of microalgae strains possessing superior industrial attributes serves to bolster the growth and productivity of the microalgae industry by mitigating production costs and reducing the time required.

The development of microalgal strains encompasses a diverse array of methodologies, including random mutagenesis and genetic engineering techniques (Park et al., 2019). Of these, genetic engineering entails direct modification of microalgal DNA to introduce or augment specific traits. Although this approach offers a speed advantage over random mutagenesis, it faces regulatory restrictions pertaining to the use of genetically modified organisms (GMOs) in many countries. Also, the application of GMOs requires high costs associated with the strain development process (transformation and selection) and downstream processing, along with regulatory considerations and biosafety concerns (Schiano di

Visconte et al., 2019). Conversely, random mutagenesis is not categorized as GMO technology, and it is characterized by its low cost and high throughput, particularly in the selection of phenotypic mutants. Therefore, the commercialization of improved strains using random mutations is more promising in terms of market demand and regulatory issues (Trovão et al., 2022). Ethyl methanesulfonate (EMS) is an alkylating agent that introduces random point mutations into DNA by guanine alkylation. EMS mutagenesis is a simple and effective method widely used in many organisms, including microalgae such as *Chlorella* sp., *Nannocloropsis* sp., and *Botryococcus* sp (Thurakit et al., 2022).

In this study, a phenotypic mutant with improved industrial traits was developed from *P. cruentum* (also known as *P. purpureum*) using EMS-induced mutagenesis. The productivity of biomass and EPS between the wild type and the phenotypic mutant was compared. The pigment contents and composition ratios between them were also compared. Furthermore, relative mRNA expression levels and wound healing effects in human skin cells were investigated, and the skin improvement effect of EPS derived from a phenotypic mutant was estimated. We also proposed a skin condition improvement mechanism of *P. cruentum*'s EPS on human skin by integrating the individual skin care mechanisms of six genes. Collectively, our findings underscore the potential of this novel *P. cruentum* mutant as a promising candidate for the large-scale production of high-value compounds.

2 Materials and methods

2.1 Preparation of wild type microalgal culture

The WT of *Porphyridium cruentum* LIMS-PS-1061 was obtained from the Library of Marine Samples of Korea. Cells were axenically maintained in an artificial seawater (ASW), according to the previous conditions (Jeon et al., 2021).

2.2 Ethyl methanesulfonate - induced mutagenesis and mutant screening

EMS (Sigma-Aldrich Co., MO, USA) was employed as a chemical mutagen to initiate random mutagenesis. Cells at the exponential stage were harvested and washed twice with distilled water (pH = 4) to eliminate excess exopolysaccharides (EPS) around the cells. Cells were resuspended in ASW supplemented with 0.5% (v/v) EMS, followed by continuous agitation for 1 h at 25°C in the dark. Then, cells were washed twice with ASW to remove excess EMS. To avert potential light-induced DNA repair, cells were incubated overnight under the same dark conditions as above. Subsequently, mutagenized cultures were spread onto 1% agar-ASW plates supplemented with 2 $\mu\text{g mL}^{-1}$ zeocin and the plates were further incubated at 25°C under constant illumination (approximately 60 $\mu\text{mol photons m}^{-2} \text{s}^{-1}$). Zeocin served as the selection marker. After 15 d, surviving colonies were separated.

2.3 Cultivation of wild type and mutants

Cells at the exponential stage were inoculated at a concentration of 0.2 g L^{-1} . Then, cells were cultivated in ASW at 25°C under constant illumination (approximately $60 \mu\text{mol photons m}^{-2} \text{ s}^{-1}$) on a rotary shaker at 120 rpm (Han et al., 2020). As a light source, white (400–700 nm) and blue (420–450 nm) light-emitting diodes (LEDs) were used (Han et al., 2021).

2.4 Analytical methods

2.4.1 Determination of algal growth

Algal growth was evaluated from cell dry weight. Cells were harvested and washed six times with distilled water ($\text{pH} = 4$), followed by filtration using a $1.2 \mu\text{m}$ glass fiber filter (GF/C; Whatman, Maidstone, UK). Subsequently, the cells were dried at 60°C until the attainment of a steady weight.

EPS extraction was performed using an alcohol precipitation method (Chen et al., 2010). The cells and culture medium were separated by centrifugation at 3500 rpm for 10 min at 4°C . Subsequently, a threefold volume of 95% (v/v) ethanol was introduced to the supernatant and the mixture was left to stand at 4°C . After a 24-h period, the mixture was centrifuged at 3500 rpm for 10 min at 4°C to separate the precipitate. The precipitate was rinsed six times with distilled water ($\text{pH} = 4$) to remove residual impurities and then lyophilized.

Pigment contents were quantified using a GENESYS 10S UV-Vis Spectrophotometer (Thermo Scientific, MA, USA). The phycobiliproteins (PBs) were extracted using the freeze-thaw method (Coward et al., 2016). The freeze-thaw cycle was repeated three times to obtain the PBs extract. The absorbances of the extracts were measured at 565 nm, 620 nm, and 650 nm using a spectrophotometer. The concentrations of phycoerythrin (PE), phycocyanin (PC), and allophycocyanin (APC) were calculated using the following equations (Munier et al., 2014):

$$\text{PE (mg L}^{-1}\text{)} = (A_{565} - 2.8 \times \text{PC} - 1.34 \times \text{APC})/12.7$$

$$\text{PC (mg L}^{-1}\text{)} = (A_{620} - 0.7 \times A_{650})/7.38$$

$$\text{APC (mg L}^{-1}\text{)} = (A_{650} - 0.19 \times A_{620})/5.65$$

Chlorophyll was extracted using an acetone extraction method (Han et al., 2019). All cells were thoroughly disrupted with 90% (v/v) acetone using a Mini-Beadbeater-16 (Biospec Products, OK, USA) to obtain the extract. Absorbances of the extracts were measured at 646 nm and 663 nm using a spectrophotometer. The concentration of chlorophyll was calculated using the following equations (Lee et al., 2016):

$$\text{Chlorophylla (mg L}^{-1}\text{)} = (12.21 \times A_{663}) - (2.81 \times A_{646})$$

2.4.2 Elemental analysis of exopolysaccharides

The elemental contents of carbon (C), hydrogen (H), nitrogen (N), and sulfur (S) in the EPS were analyzed using a Vario-Micro

Cube (Elementar Analysensysteme GmbH, Hanau, Germany). The analysis was performed on completely lyophilized EPS. The weight percentage (Wt%) of each element was evaluated for 1.8 mg of a sample at 1150°C . The sulfanilic acid served as the standard for this analysis.

2.4.3 Assessing the bioactivity of exopolysaccharides

The completely lyophilized EPS derived from PPE was used. EPS was dissolved in distilled water to a concentration of 4 mg mL^{-1} . Then, the EPS solution was diluted to 0.1% (v/v; 4 ppm) and 1% (v/v; 40 ppm) and used for analysis.

2.4.3.1 Human cell culture

Immortalized human keratinocytes (HaCaT) and human dermal fibroblast (Hs68) were obtained from American Type Culture Collection (VA, USA) and cultured in Dulbecco's Modified Eagle Medium (DMEM; HyClone Laboratories, Inc., UT, USA) containing 10% (v/v) fetal bovine serum (FBS; HyClone Laboratories, Inc., UT, USA) and 1% (v/v) antibiotic-antimycotic (AA; HyClone Laboratories, Inc., UT, USA) solution at 37°C in a 5% (v/v) CO_2 atmosphere. When the cells reached about 80% confluence, cells were subcultured using a solution of 4-(2-hydroxyethyl)-1-piperazine ethanesulfonic acid-buffered saline and trypsin/ethylenediaminetetraacetic acid (EDTA).

2.4.3.2 RNA extraction and real-time RT-PCR analysis

To evaluate the skin benefits of EPS, the expression levels of aquaporin 3 (AQP3), filaggrin (FLG), involucrin (IVL), and loricrin (LOR) were assessed in epidermal cells (HaCaT), while elastin (ELN) and fibrillin-1 (FBN) were evaluated in dermal cells (Hs68). HaCaT and Hs68 cells were harvested after 24 h of treatment with EPS. Retinoic acid, adipoRon, and epigallocatechin gallate (EGCG) were purchased from Sigma Aldrich (MO, USA) and used as positive controls. Total RNA was isolated using TRIzol reagent (TaKaRa, Shiga, Japan) according to the manufacturer's instructions. Approximately $2 \mu\text{g}$ of total RNA was synthesized to cDNA using Reverse Transcription Premix (Elpis-biotech, Daejeon, Korea). Gene expression levels were quantified, and the data were analyzed using the StepOne Plus™ system software (Applied Biosystems, CA, USA). Real-time RT-qPCR amplification reactions were performed using SYBR Green PCR Master Mix with premixed ROX (Applied Biosystems, CA, USA). The following primer pairs (Bioneer, Daejeon, Korea) were used in the reactions, which were performed on an ABI 7300 instrument accordance with the manufacturer's protocol (Applied Biosystems, CA, USA): β -actin (F: 5'-GGCCATCTCTTGCTCGAAGT-3' and R: 5'-GACACCTTCAACACCCAGC-3'), AQP 3 (F: 5'-GTCACCTCTGGGCA TCCTCAT-3' and R: 5'-CTATTCCAGCACCCAAGAAGG-3'), FLG (F: 5'-AGTGCACCTCAGGGGGCTCACA-3' and R: 5'-CCG GCTTGCCGTAATGTGT-3'), IVL (F: 5'-TGAAACAGCCAAC TCCACTG-3' and R: 5'-GGAGCTCCAACAGTTGCTCT-3'), LOR (F: 5'-AATAGATCCCCCAGGGTACCA-3' and R: 5'-CGGTGCCCTGGAAAAC-3'), ELN (F: 5'-CACCTTGCCC TTGTAGAATCCA-3' and R: 5'-CCATGACAGGTCAACCAGG TT-3'), FBN1 (F: 5'-AATGTCAGACGAAGCCAGGG-3' and R:

5'-GATTTGGTGACGGGGTTCCT-3'). The mRNA expression of β -actin was used as an internal control.

2.4.3.3 Fibroblast migration assay

Hs68 cells (2×10^4 cells well⁻¹) were seeded into IncuCyte[®] ImageLock 96-well plates (Essen BioScience, MI, USA) at almost 100% confluence and incubated in an atmosphere of 5% CO₂ at 37°C overnight. Cells were scratched by the IncuCyte[®] WoundMaker tool (Essen BioScience, MI, USA) to create precise, uniform cell-free zones. And then, the EPS was treated into the cells with FBS-free DMEM media, and the cell plate was placed into the IncuCyte Live-Cell Analysis System (Essen BioScience, MI, USA) to allow the plate to be warmed to 37°C for 30 min prior to scanning. Wound closure was monitored by taking digitized images of the culture fields every 2 h for up to 16 h after scratching. The images were captured and analyzed using the IncuCyte Live-Cell Analysis System.

2.5 Statistical analysis

Each experiment was conducted with at least three independent specimens. One-way analysis of variance (ANOVA) with Tukey's tests was performed for statistical analysis using SAS 9.4 software. The p-value of < 0.05 was considered to be statistically significant. The data are presented as mean values \pm standard error (SE).

3 Results and discussion

3.1 Changes in growth parameters between wild type and phycobiliprotein production-enhancing mutant

Ethyl methanesulfonate (EMS)-induced mutagenesis and zeocin selection were employed for the development and screening of *P. cruentum* mutants. EMS-induced mutagenesis is a simple and cost-effective method to generate extensive mutations.

However, since EMS generates random mutations, considerable time and effort are required to isolate only specific mutants in which DNA is extensively altered. Zeocin is an antibiotic to which numerous species of microalgae present sensitivity (Osorio et al., 2019). Also, zeocin can act as a mutagen that induces mutations in microalgae (Lin et al., 2017). Therefore, zeocin was used as a subsequent mutagen and selection marker. The mutant was selected based on colony size on zeocin-containing agar medium and subsequent experiments were performed.

Differences in growth parameters between the WT and the mutant were compared under white light and blue light conditions. Under white light conditions, the cell dry weight of the mutant (0.854 g L⁻¹) increased by 33.9% compared to the WT (0.638 g L⁻¹) (Figure 1A). Under blue light conditions, however, there was no significant difference between the cell dry weights of the mutant (0.736 g L⁻¹) and the WT (0.756 g L⁻¹). Additionally, there was no significant difference in the yield of exopolysaccharides (EPS) between the WT and the mutant under both conditions (Figure 1B). Interestingly, the mutant exhibited prominent cell growth under white light conditions, while the WT exhibited prominent cell growth under blue light conditions. Various factors such as light source, temperature, pH, salinity, and the availability of nutrients influence the cellular growth of microalgae (Lee et al., 2015; Srinuanpan et al., 2018). Among these, the light source is considered the most critical factor influencing cell growth. Photosynthesis is a fundamental process through which microalgae produce energy, and this process is heavily reliant on light. The intensity, quality, and photoperiod of the light source can profoundly impact the photosynthetic efficiency in microalgae, with the energy generated being vital for cell growth and reproduction (Kwan et al., 2021). In addition, microalgae collect light through antenna pigments and convert it into energy. Microalgae possess a diversity of pigments, which are categorized into primary and accessory pigments, each absorbing light within a specific wavelength range and exerting a significant influence on cell growth (Sirisuk et al., 2018). Moreover, light is not just instrumental in energy production but also plays a critical role in the

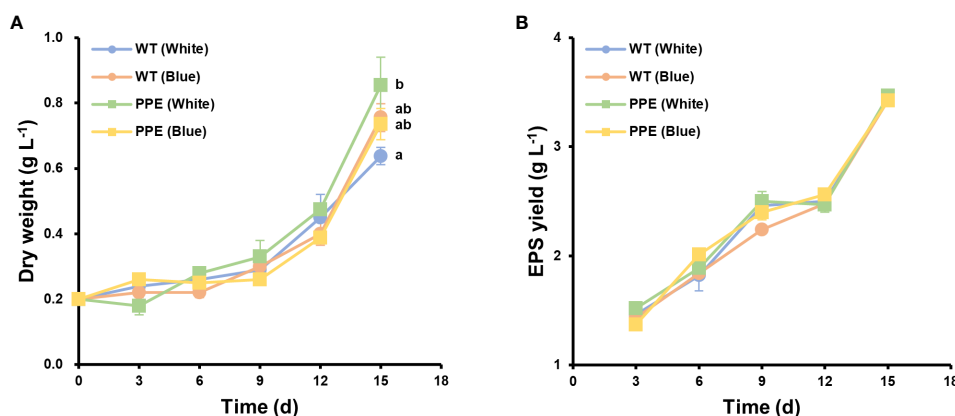


FIGURE 1

Differences in cell growth between wild type (WT) and the strain PPE. (A) The dry weight of WT and PPE. (B) Exopolysaccharides (EPS) yield of WT and PPE. White and Blue indicate incubation under white and blue LEDs, respectively. There was no statistically significant difference in EPS yield. Data are shown as mean \pm standard error (n = 3). Each lowercase letter indicates a group that is statistically distinct.

physiological regulation of microalgae. For instance, variations in light intensity and duration can have direct effects on the cell cycle as well as various metabolic pathways (Jaubert et al., 2017). In this experiment, all other environmental factors were kept constant except for the light source. Therefore, based on the observed cell growth results, it can be inferred that alterations in pigment occurred in the mutant.

Fascinating changes in pigment were observed between the WT and mutant. There was no statistically significant difference in the total amount of major pigments (chlorophyll and phycobiliproteins, referred to as 'PBs') between the WT and mutant under white light conditions (Figure 2A). Under white light, the total amounts of major pigments in the WT and mutant were 7.80 mg g⁻¹ and 8.06 mg g⁻¹, respectively. Under blue light conditions, the total amount of major pigments in the WT and mutant significantly increased to 12.7 mg g⁻¹ and 11.4 mg g⁻¹, respectively, but there was no statistical difference between them. However, despite the total amount of pigment being similar, the composition of pigments exhibited a dramatic difference. Under white light, the chlorophyll content in the mutant was 1.74 mg g⁻¹, which was 2.20 times lower than that of the WT (3.83 mg g⁻¹) (Figure 2A). In contrast, the phycobiliproteins (PBs) content in the mutant was 6.33 mg g⁻¹, which was 1.59 times higher than that of the WT (3.97 mg g⁻¹). Similarly, under blue light, the chlorophyll content in the mutant was 1.25 mg g⁻¹, which was 3.61 times lower than that of the WT (4.50 mg g⁻¹), while the PBs content was 10.1 mg g⁻¹, which was 1.23 times higher than that of the WT (8.22 mg g⁻¹). Based on these remarkable differences in pigment content, the mutant was designated as a phycobiliprotein production-enhancing mutant (PPE).

To investigate the pigment composition profiles in greater detail, the contents of chlorophyll, phycoerythrin (PE), phycocyanin (PC), and allophycocyanin (APC) in the WT and PPE were analyzed (Figures 2A, B). The significant increase in PB content in PPE was primarily attributed to increases in APC and

PC. Under white light, the contents of APC and PC in PPE increased by 2.23- and 1.63-fold, respectively, compared to the WT, while PE increased only by 1.07-fold. The weight percentages of PBs in the total amount of major pigment in WT and PPE were 50.9% and 78.5%, respectively. Similarly, under blue light, the contents of APC, PC, and PE in PPE increased by 1.28-, 1.20-, and 1.18-fold, respectively, compared to the WT. The weight percentages of PBs in the total amount of major pigment in WT and PPE were 64.6% and 89.0%, respectively. These alterations in pigment composition between WT and PPE are presumed to be a consequence of chlorophyll deficiency. In *P. cruentum*, chlorophyll and PBs have a complementary relationship. It is known that a deficiency in chlorophyll promotes the production of PBs as a compensatory mechanism to maintain the photosynthetic capacity of cells (Jeon et al., 2021). In addition, the increase in PBs observed in both WT and PPE under blue light is inferred as a defense mechanism against stress induced by blue light. Blue light has a short wavelength (typically 380–500 nm) and has higher energy photons than are required for photosynthesis (Schulze et al., 2014). Excess photon energy can cause photooxidative damage to cells due to the generation of reactive oxygen species (ROS) (Coward et al., 2016). In *P. cruentum*, PBs play a role in scavenging ROS (Peña-Medina et al., 2023). It has been demonstrated that PE acts through the primary pathway by directly sequestering ROS and possesses high reducing power. In contrast, PC and APC function through both primary and secondary pathways, notably serving as chelators of metal ions that are involved in ROS synthesis (Sonani et al., 2015). Indeed, it has been reported that PB production is enhanced for stress reduction in *Porphyridium* sp. under blue light (Coward et al., 2016; Huang et al., 2021).

These results support our hypothesis that the difference in cell growth between WT and PPE was due to variations in pigment composition. In *P. cruentum*, chlorophyll absorbs light at 400–500 nm and 650–720 nm (Dagnino-Leone et al., 2022), while PE absorbs at 490–570 nm (Sepúlveda-Ugarte et al., 2011), PC at 550–650 nm

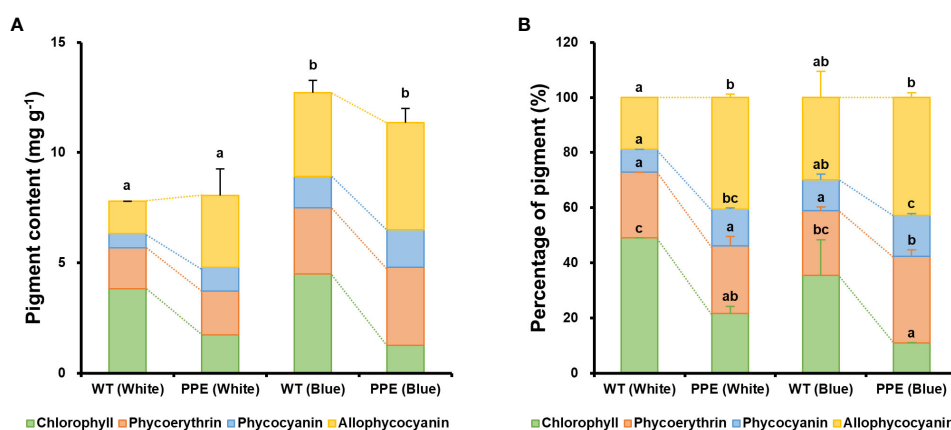


FIGURE 2

Changes in major pigment content between wild type (WT) and the strain PPE. (A) Amounts of the four major pigments per cell dry weight. (B) Percentages of the four major pigments. The dotted line represents the change in pigment content between WT and PPE under the same culture conditions. White and Blue indicate incubation under white and blue LEDs, respectively. The error bars and significance shown in (A) represent the results for the total amount of pigment, while the error bars and significance shown in (B) represent the results for the ratio of each pigment. Data are shown as mean \pm standard error ($n = 3$). Each lowercase letter indicates a group that is statistically distinct.

(Ma et al., 2008), and APC at 600–680 nm (Dagnino-Leone et al., 2020). The wavelengths of the white and blue LEDs used in the experiment were 400–700 nm and 420–450 nm, respectively. In terms of photosynthetic pigments, PBs have the capacity to absorb light across a broad spectrum (490–680 nm), allowing them to support photosynthesis by absorbing light in ranges where chlorophyll absorption is less efficient (500–650 nm) (Watanabe and Ikeuchi, 2013). Furthermore, in *P. cruentum*, light energy is sequentially transmitted along the pathways of PE, PC, APC, and chlorophyll a, with electron flow correlating with the quantity of PBs (Yokono et al., 2011). Consequently, cell growth in PPE was more pronounced than that of WT under white light conditions. On the other hand, interestingly, there was no significant difference in cell growth between WT and PPE under blue light, despite chlorophyll being more adept at absorbing blue light compared to PBs. As previously mentioned, it is inferred that this is due to the high energy levels of blue light and the stress-reducing effects of PBs. Blue light is absorbed by chlorophyll and utilized for cellular energy metabolism through photosynthesis, but it also acts as a stress-inducing factor that can inhibit cell growth. Under blue light, WT possesses a higher light energy conversion efficiency than PPE, owing to its higher chlorophyll content. Conversely, PPE exhibits higher stress resistance due to its higher PB content compared to WT. In other words, under blue light, WT has high light absorption efficiency but low stress tolerance, whereas PPE has high stress tolerance but low light absorption efficiency. Consequently, no significant difference in cell growth was observed between PPE and WT under blue light conditions. These results imply that the relationship between pigment and cell growth in microalgae involves the collective action of several pigments rather than the isolated function of individual pigments, and both light absorption efficiency and light inhibition should be taken into account.

3.2 Assessment of skin improvement potential of exopolysaccharides derived from phycobiliproteins production-enhancing mutant

A subsequent analysis was conducted on the EPS produced from PPE to ascertain its industrial potential. The EPS originated from *P. cruentum* is primarily composed of sulfated polysaccharides (SPs) and exhibits biological activities such as antioxidant, anti-inflammatory, anti-cancer, and UV protective properties, making it a valuable biological material in the cosmetic and medical industries (Li et al., 2019). Also, the biological activity of EPS is generally positively correlated with its sulfur content (Lieberman et al., 2020). Elemental analysis revealed no significant differences in the weight percentages of carbon (C), hydrogen (H), and sulfur (S) between the EPS produced from WT and PPE (Figure 3). The weight percentages of C, H, and S in the EPS derived from WT were $0.243 \pm 0.028\%$, $0.848 \pm 0.047\%$, and $14.3 \pm 0.7\%$, respectively. The weight percentages of C, H, and S in the EPS derived from PPE were $0.485 \pm 0.100\%$, $0.817 \pm 0.003\%$, and $12.6 \pm 0.4\%$, respectively. On the other hand, nitrogen (N) was not detected in both EPS, indicating that cell debris

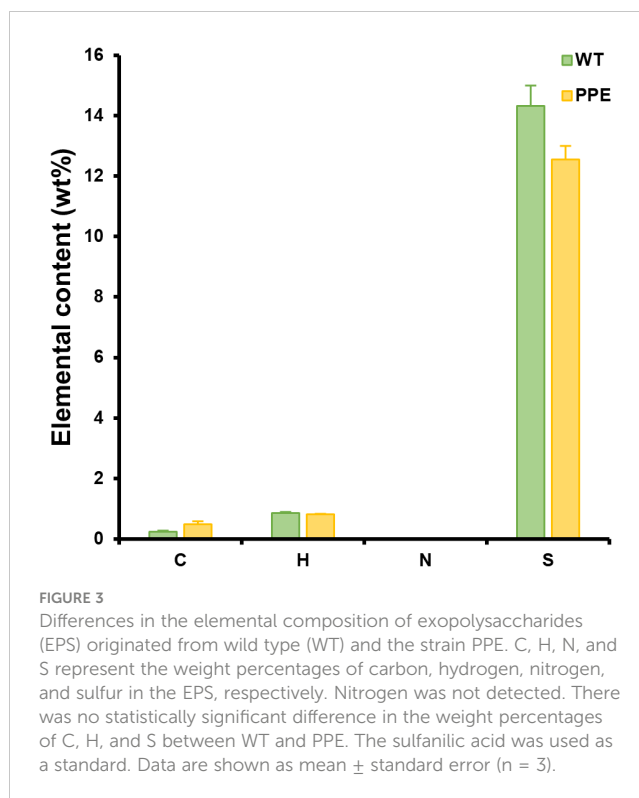


FIGURE 3
Differences in the elemental composition of exopolysaccharides (EPS) originated from wild type (WT) and the strain PPE. C, H, N, and S represent the weight percentages of carbon, hydrogen, nitrogen, and sulfur in the EPS, respectively. Nitrogen was not detected. There was no statistically significant difference in the weight percentages of C, H, and S between WT and PPE. The sulfanilic acid was used as a standard. Data are shown as mean \pm standard error (n = 3).

(especially lipids and proteins) and nucleic acids were absent from the extracted EPS. Despite the slight difference in weight percentage, an analysis of variance (ANOVA) revealed that these differences in the elemental compositions of both EPS were not statistically significant. These results suggest that the EPS produced from PPE likely has biological activity comparable to that of EPS from WT. Thus, the potential for skin improvement of EPS produced from PPE was evaluated in human skin cells.

Since AQP3, FLG, IVL, and LOR are all expressed in keratinocytes and play roles in water transport, hydration, and skin barrier formation, changes in the expression of these genes were investigated in epidermal cells (HaCaT). In contrast, ELN and FBN, which are fibrous proteins involved in maintaining skin elasticity, are produced in dermal fibroblasts; therefore, changes in the expression of these genes were evaluated in dermal cells (Hs68). The results of the real-time RT-PCR analysis showed that EPS could potentially be used for skin improvement (Figure 4). Expression levels of aquaporin 3 (AQP3) in the EPS-treated groups were 1.66- and 2.80-fold higher at concentrations of 4 ppm and 40 ppm respectively, compared to the control (Figure 4A). In addition, expression levels of filaggrin (FLG) in the EPS-treated groups were 1.72- and 3.23-fold higher at concentrations of 4 ppm and 40 ppm respectively, compared to the control (Figure 4B). Retinoic acid, used as a positive control, exhibited AQP3 and FLG expression levels that were 2.30- and 1.72-fold higher, respectively, compared to the control. AQP3 and FLG are two pivotal proteins that play crucial roles in skin moisturization. AQP3, a water channel protein located in the cell membranes of skin cells, facilitates the transport of moisture, helping to maintain the moisture content of the skin (Bollag et al., 2020). Also, AQP3 has a glycerol transport capability, so it plays an important role in strengthening the

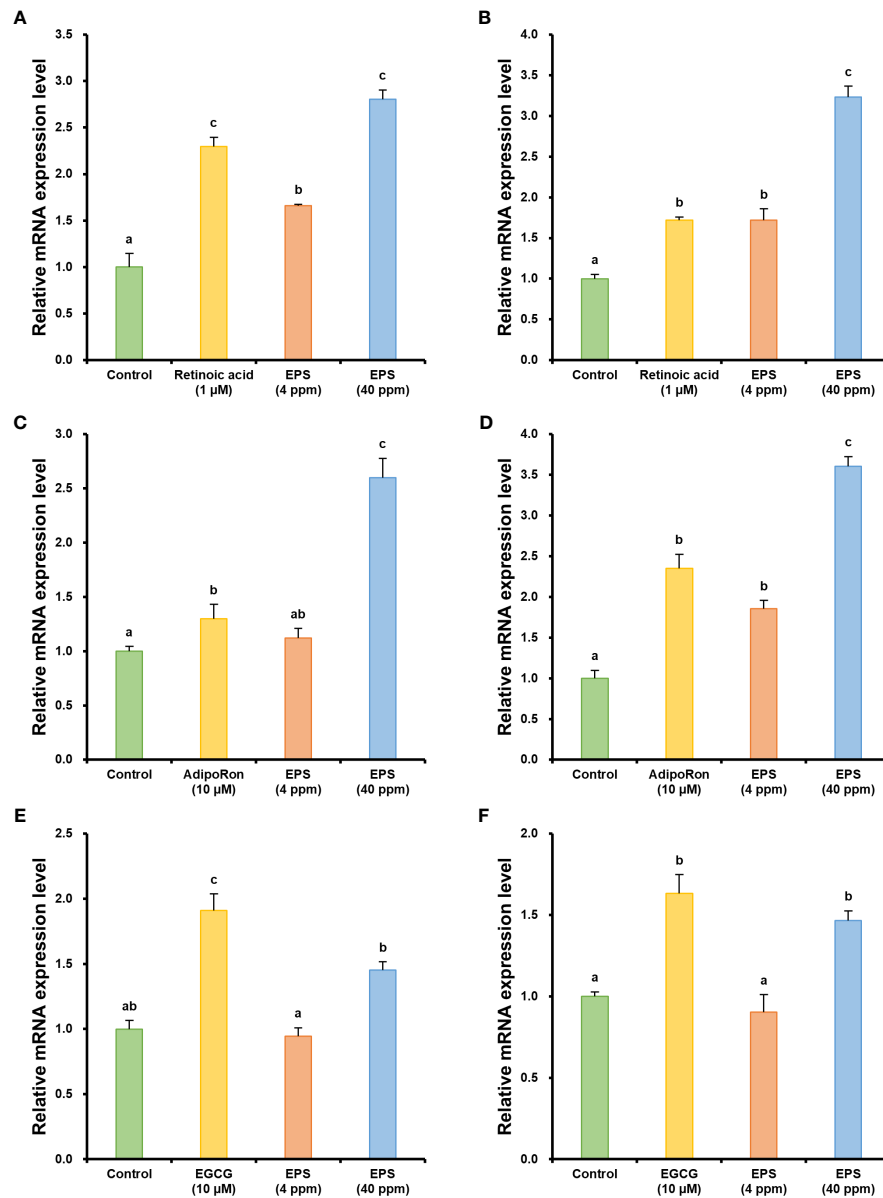


FIGURE 4

Changes in relative mRNA expression levels of genes related to skin moisturization, barrier enhancement, and elasticity improvement. (A) Relative mRNA expression of aquaporin 3. (B) Relative mRNA expression of filaggrin. (C) Relative mRNA expression of involucrin. (D) Relative mRNA expression of lorcinin. (E) Relative mRNA expression of elastin. (F) Relative mRNA expression of fibrillin-1. The human cells were harvested 24 h after treatment with phycobiliprotein production-enhancing mutant-derived exopolysaccharides (EPS). The mRNA expression of β -actin was used as an internal control. Retinoic acid, adipoRon, and epigallocatechin gallate (EGCG) were used as a positive control. Data are shown as mean \pm standard error ($n = 3$). Each lowercase letter indicates a group that is statistically distinct.

moisturizing and barrier functions of the skin. FLG, which is present in the epithelial layer of the skin, enhances the adhesion between skin cells, minimizing water loss and protecting the skin against external stimuli (Kim et al., 2012). Also, FLG is involved in the production of natural moisturizing factors within the skin. Thus, an increase in the gene expression levels of AQP3 and FLG suggests an enhancement of skin moisturization.

In addition to FLG, the expression levels of involucrin (IVL) and lorcinin (LOR), which are related to skin barrier enhancement, were also analyzed. The expression levels of IVL were 1.12- and 2.60-fold higher in the EPS-treated groups at concentrations of 4 ppm and 40

ppm, respectively, compared to the control (Figure 4C). In addition, the expression levels of LOR were 1.86- and 3.60-fold higher in the EPS-treated groups at concentrations of 4 ppm and 40 ppm, respectively, compared to the control (Figure 4D). AdipoRon was used as a positive control and exhibited 1.30-fold higher IVL and 2.35-fold higher LOR expression levels than the control. IVL is a protein present in the epithelial cells of the skin and is one of the principal components involved in forming the keratinized epidermis, which serves as a protective barrier in the skin (Furue et al., 2015). IVL functions as a scaffold for the formation of the keratinized epidermis by cross-linking with other proteins through the catalytic action of an enzyme known as

transglutaminase. LOR is another essential protein of the keratinized epidermis, which constitutes a significant part of the keratinized epidermis and is involved in the aggregation of keratin fibers (Furue et al., 2015). This aggregation and subsequent cross-linking result in a densely packed protective layer that is highly resistant to mechanical stress, thereby contributing to skin barrier enhancement. Thus, an increase in the gene expression levels of IVL and LOR is intimately associated with the strengthening of the skin barrier.

Subsequently, the expression levels of elastin (ELN) and fibrillin-1 (FBN1), which are associated with the improvement of skin elasticity, were analyzed. When treated with 40 ppm of EPS, the expression levels of ELN and FBN1 were 1.45- and 1.47-fold higher, respectively, compared to the control (Figures 4E, F). No statistical significance was observed when both genes were treated with 4 ppm of EPS. These results suggest that an improvement in skin elasticity can be expected when treated with EPS of a certain concentration or higher. Epigallocatechin gallate (EGCG) was used as a positive control and exhibited 1.91-fold and 1.63-fold higher expression levels of ELN and FBN1, respectively, compared to the control. ELN encodes elastin, which is a key protein in the skin that provides elasticity. Elastin allows the skin to stretch and then return to its original shape (Romana-Souza et al., 2020). As elastin levels decrease with age, the skin loses its ability to regain its shape, leading to sagging and wrinkles. In addition, FBN1 encodes fibrillin-1, a component of microfibrils that plays a crucial role in maintaining skin elasticity and structure (Romana-Souza et al., 2020). Moreover, fibrillin-1 interacts with elastin, aiding in the

support of the skin's microstructure, and helps the skin withstand physical stress, such as stretching. Thus, an increase in the expression levels of the ELN and FBN1 genes can contribute to improved skin elasticity and structural reinforcement, which can help slow down the aging of the skin and reduce wrinkles.

Finally, a scratch assay was conducted on Hs68 cells to test the ability of EPS to promote cell migration, which is related to wound healing (Figure 5). In the absence of any treatment, the cells spontaneously migrated to induce re-epithelialization. Interestingly, when the cells were treated with EPS at a concentration of 40 ppm, a significant enhancement in wound closure was observed (Figure 5A). Indeed, the wound recovery rate after 16 hours was 54.7% with EPS treatment, which was significantly higher than that of EGCG (46.3%) used as a positive control, or untreated cells (control; 40.3%) (Figure 5B). Moreover, it was also confirmed that EPS has the potential to enhance the skin absorption rate of other skin active ingredients (Supplementary Figure S1). These results demonstrate the potential of EPS derived from PPE for skin improvement and suggest that it can be applied in the cosmetic or medical industry.

3.3 Suggested role of *Porphyridium cruentum*-derived exopolysaccharides in improving human skin condition

Integrating the aforementioned results, we estimated the mechanism through which EPS derived from *P. cruentum* improves

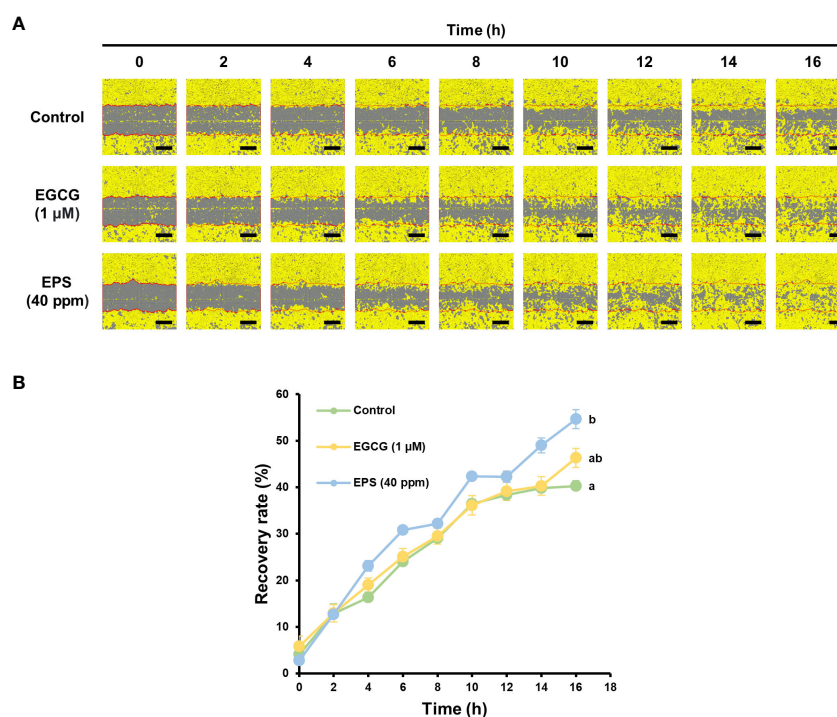


FIGURE 5

The evaluation of fibroblast migration for wound healing. (A) The scratch test of Hs68 cells. (B) The recovery rates in the scratch test. Wound closure was monitored by taking digitized images of culture fields every 2 h after scratching. Exopolysaccharides (EPS) derived from the phycobiliprotein production-enhancing mutant were used. The epigallocatechin gallate (EGCG) was used as a positive control. The scale bars = 400 μm. Data are shown as mean ± standard error (n = 3).

the condition of human skin cells (Figure 6). The EPS was found to enhance skin moisturization, elasticity, barrier enhancement, and wound healing through the upregulation of six genes.

Aquaporin-3 (AQP3), a membrane transporter of water and glycerol, is expressed in the plasma membrane of basal keratinocytes in normal skin epidermis. This transporter plays a pivotal role in the stratum corneum's (SC) water retention, elasticity, and biosynthesis. Notably, glycerol transport by AQP3 is more critical than water transport for skin physiology and phenotype alterations (Hara-Chikuma and Verkman, 2005). AQP3 enhances skin moisturization and elasticity by increasing glycerol content, a key determinant of skin hydration. Additionally, AQP3 facilitates re-epithelialization, an essential stage in wound healing, by promoting keratinocyte migration and proliferation from the surrounding epidermis and appendages such as hair follicles and sweat glands. The water and glycerol transport facilitated by AQP3 enhances keratinocyte migration and proliferation, respectively (Hara-Chikuma and Verkman, 2008). Increased glycerol contents due to AQP3 not only aid in skin barrier recovery but also contribute to the enhancement of epidermal barrier functions (Hara and Verkman, 2003). In summary, AQP3-facilitated water transport is involved in accelerating wound healing, also its glycerol transport contributes to skin hydration and elasticity, as well as cell proliferation.

Natural moisturizing faction (NMF) is a key factor in maintaining skin moisture, is present in keratinocytes, and contributes to both moisture retention and epidermal barrier functions. NMF, synthesized from filaggrin (FLG) in the SC, typically comprises amino acids (40%), pyrrolidone carboxylic acid (PCA, 12%), lactate (12%), and urea (7%). Its synthesis follows a

sequence of processes (Tsukui et al., 2022): FLG is initially produced by the precursor protein profilaggrin (proFLG), which is metabolized to FLG through dephosphorylation and other mechanisms, subsequently binding with keratin in keratinocytes. In the upper SC, proteolytic enzymes degrade FLG from keratin. The arginine in FLG is citrullinated (Cit) by the protein arginine deiminase, and Cit residues are released and then fragmented into amino acids by bleomycin hydrolase. These amino acids are further transformed by degradative enzymes, with Glu and Gln converting into PCA, His into urocanic acid, and Arg into urea (Tang et al., 2016). Additionally, mammalian epidermal cells feature a cornified cell envelope (CE), a 15 nm thick protein layer cross-linked by isopeptide and disulfide bonds. FLG, along with involucrin (IVL) and loricrin (LOR), forms this complex structure. The human epidermal CE comprises 65–70% LOR, about 10% FLG and cysteine-rich protein (CRP), and 2–5% IVL, small proline-rich proteins (SPRRs), and cystatin A (Tharakan et al., 2010). The formation of CE *in vivo* is a multistage process, starting with the initial attachment of IVL, SPRR, CRP, and cystatin A to the cell membrane, followed by a heavy deposition of LOR with some FLG. In summary, an increase in FLG expression enhances NMF biosynthesis, thereby strengthening the SC's capacity for moisture retention. FLG also collaborates with IVL and LOR in forming the CE, further strengthening epidermal barrier functionality and moisture retention.

Elastic fibers are a crucial component of the extracellular matrix, imparting stretchability, resilience, and cellular interaction to a wide range of elastic tissues. Elastin (ELN) constitutes the majority of elastic fibers and is formed by the hierarchical assembly of its monomer, tropoelastin (Ozsvar et al., 2021). Fibrillin microfibrils, extensible polymers present in both elastic and non-

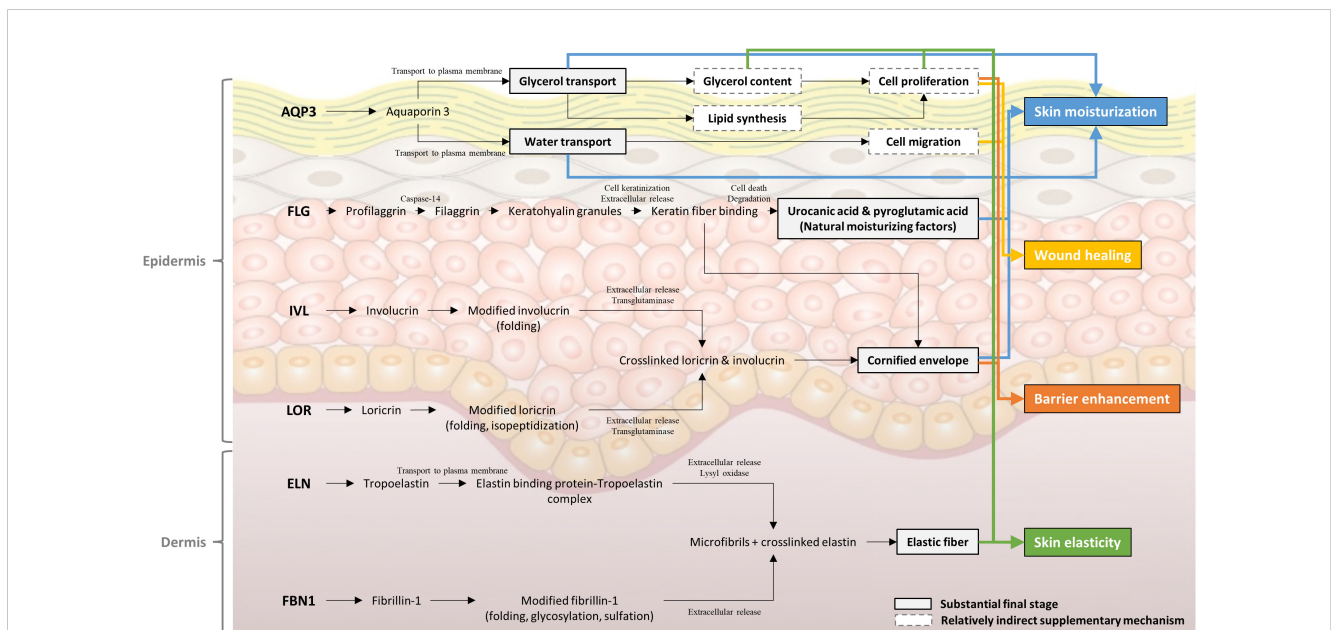


FIGURE 6 Proposed mechanisms for *Porphyridium cruentum* exopolysaccharides-dependent skin hydration, wound healing, barrier enhancement, and skin elasticity improvement.

elastic tissues, provide long-range elasticity to connective tissue. These microfibrils also act as a scaffold for elastin deposition during elastic fiber synthesis, playing a vital role in maintaining tissue integrity (Ramirez and Sakai, 2010). In elastic fiber assembly, elastin globules are directly deposited onto microfibril templates, forming elastic fiber composed of an amorphous elastin central core surrounded by a fibrillin microfibril sheath (Thomson et al., 2019). An increase in the expression of both ELN and FBN1, therefore, leads to an enhanced biosynthesis of elastic fibers, significantly contributing to the improvement of skin elasticity.

In summary, EPS derived from *P. cruentum* enhances skin moisturization, elasticity, barrier enhancement, and wound healing. This improvement is mediated through the individual or synergistic effects of six key genes implicated in skin health: (1) AQP3 enhances skin hydration, elasticity, wound healing, and barrier function. (2) FLG contributes to skin hydration. (3) FLG, IVL, and LOR jointly improve skin hydration and barrier function. (4) ELN and FBN1 play a significant role in enhancing skin elasticity.

This research introduces a mutant strain of *P. cruentum*, developed through EMS-induced mutagenesis, which exhibits superior industrial traits. This study further elucidates the relationship between pigment and cell growth in *P. cruentum* and the mechanisms by which EPS derived from *P. cruentum* ameliorates skin conditions. Given its skin care and pharmacological properties, EPS from *P. cruentum* is poised for varied industrial applications. Consequently, we anticipate that our findings will have broad implications and utility across industries utilizing *P. cruentum*.

4 Conclusion

In this study, an ethyl methanesulfonate (EMS)-induced mutant of *Porphyridium cruentum* was developed, exhibiting enhanced growth rates and phycobiliprotein content. This mutant, termed phycobiliprotein production-enhancing mutant (PPE), displayed variations in pigment composition, which influenced cell growth via light absorption, energy conversion, and stress reduction. Additionally, PPE-derived exopolysaccharides (EPS), similar in composition to the wild type, showed potential for skin improvement through real-time RT-PCR and fibroblast migration assays. By integrating the mechanisms of six genes related to skin care, a mechanism by which *P. cruentum* EPS affects skin hydration, wound healing, barrier enhancement, and skin elasticity improvement was proposed. The study provides insight into the pigment-cell growth relationship in *P. cruentum* and an understanding of the mechanisms by which *P. cruentum* EPS improves skin conditions.

Data availability statement

The raw data supporting the conclusions of this article will be made available by the authors, without undue reservation.

Ethics statement

Ethical approval was not required for the studies on humans in accordance with the local legislation and institutional requirements because only commercially available established cell lines were used.

Author contributions

S-IH: Conceptualization, Formal analysis, Investigation, Validation, Visualization, Writing – original draft, Writing – review & editing. YH: Formal analysis, Investigation, Validation, Visualization, Writing – original draft, Writing – review & editing. MJ: Conceptualization, Formal analysis, Investigation, Validation, Visualization, Writing – original draft. SYK: Investigation, Writing – original draft. SHK: Investigation, Writing – original draft. S-JK: Funding acquisition, Project administration, Writing – review & editing. JR: Project administration, Writing – review & editing. JK: Project administration, Writing – review & editing. J-WA: Project administration, Supervision, Writing – review & editing.

Funding

The author(s) declare financial support was received for the research, authorship, and/or publication of this article. This work was supported by the research program (No. 523410-24) of KAERI, Republic of Korea. This work was also supported by the National Research Foundation of Korea (NRF) grant funded by the Korea government (RS-2022-00156231).

Conflict of interest

The authors declare that the research was conducted in the absence of any commercial or financial relationships that could be construed as a potential conflict of interest.

Publisher's note

All claims expressed in this article are solely those of the authors and do not necessarily represent those of their affiliated organizations, or those of the publisher, the editors and the reviewers. Any product that may be evaluated in this article, or claim that may be made by its manufacturer, is not guaranteed or endorsed by the publisher.

Supplementary material

The Supplementary Material for this article can be found online at: <https://www.frontiersin.org/articles/10.3389/fmars.2024.1365311/full#supplementary-material>

References

- Andrew, M., and Jayaraman, G. (2021). Marine sulfated polysaccharides as potential antiviral drug candidates to treat Corona Virus disease (COVID-19). *Carbohydr. Res.* 505, 108326. doi: 10.1016/j.carres.2021.108326
- Ashaolu, T. J., Samborska, K., Lee, C. C., Tomas, M., Capanoglu, E., Tarhan, Ö., et al. (2021). Phycocyanin, a super functional ingredient from algae; properties, purification characterization, and applications. *Int. J. Biol. Macromol.* 193, 2320–2331. doi: 10.1016/j.ijbiomac.2021.11.064
- Bollag, W. B., Aitkens, L., White, J., and Hyndman, K. A. (2020). Aquaporin-3 in the epidermis: more than skin deep. *Am. J. Physiol.-Cell Physiol.* 318, C1144–C1153. doi: 10.1152/ajpcell.00075.2020
- Casas-Arrojo, V., Decara, J., de los Angeles Arrojo-Agudo, M., Pérez-Manriquez, C., and Abdala-Díaz, R. T. (2021). Immunomodulatory, antioxidant activity and cytotoxic effect of sulfated polysaccharides from *Porphyridium cruentum* (sf Gray) Nägeli. *Biomolecules* 11, 488. doi: 10.3390/biom11040488
- Chen, B., You, W., Huang, J., Yu, Y., and Chen, W. (2010). Isolation and antioxidant property of the extracellular polysaccharide from *Rhodella reticulata*. *World J. Microbiol. Biotechnol.* 26, 833–840. doi: 10.1007/s11274-009-0240-y
- Coward, T., Fuentes-Grünwald, C., Silkina, A., Oatley-Radcliffe, D. L., Llewellyn, G., and Lovitt, R. W. (2016). Utilising light-emitting diodes of specific narrow wavelengths for the optimization and co-production of multiple high-value compounds in *Porphyridium purpureum*. *Bioresour. Technol.* 221, 607–615. doi: 10.1016/j.biortech.2016.09.093
- Dagnino-Leone, J., Figueroa, C. P., Castañeda, M. L., Youlton, A. D., Vallejos-Almirall, A., Agurto-Muñoz, A., et al. (2022). Phycobiliproteins: Structural aspects, functional characteristics, and biotechnological perspectives. *Comp. Struct. Biotechnol. J.* 20, 1506–1527. doi: 10.1016/j.csbj.2022.02.016
- Dagnino-Leone, J., Figueroa, M., Uribe, E., Hinrichs, M. V., Ortiz-López, D., Martínez-Oyanedel, J., et al. (2020). Biosynthesis and characterization of a recombinant eukaryotic allophycocyanin using prokaryotic accessory enzymes. *MicrobiologyOpen* 9, e989. doi: 10.1002/mbo3.989
- Furue, M., Tsuji, G., Mitoma, C., Nakahara, T., Chiba, T., Morino-Koga, S., et al. (2015). Gene regulation of flaggrin and other skin barrier proteins via aryl hydrocarbon receptor. *J. Dermatol. Sci.* 80, 83–88. doi: 10.1016/j.jdermsci.2015.07.011
- Han, S.-I., Jeon, M. S., Heo, Y. M., Kim, S., and Choi, Y.-E. (2020). Effect of *Pseudoalteromonas* sp. MEBiC 03485 on biomass production and sulfated polysaccharide biosynthesis in *Porphyridium cruentum* UTEX 161. *Bioresour. Technol.* 302, 122791. doi: 10.1016/j.biortech.2020.122791
- Han, S.-I., Jeon, M. S., Park, Y. H., Kim, S., and Choi, Y.-E. (2021). Semi-continuous immobilized cultivation of *Porphyridium cruentum* for sulfated polysaccharides production. *Bioresour. Technol.* 341, 125816. doi: 10.1016/j.biortech.2021.125816
- Han, S.-I., Yao, J., Lee, C., Park, J., and Choi, Y.-E. (2019). A novel approach to enhance astaxanthin production in *Haematococcus lacustris* using a microstructure-based culture platform. *Algal Res.* 39, 101464. doi: 10.1016/j.algal.2019.101464
- Hara, M., and Verkman, A. (2003). Glycerol replacement corrects defective skin hydration, elasticity, and barrier function in aquaporin-3-deficient mice. *Proc. Natl. Acad. Sci. U.S.A.* 100, 7360–7365. doi: 10.1073/pnas.1230416100
- Hara-Chikuma, M., and Verkman, A. (2005). Aquaporin-3 functions as a glycerol transporter in mammalian skin. *Biol. Cell.* 97, 479–486. doi: 10.1042/BC20040104
- Hara-Chikuma, M., and Verkman, A. (2008). Roles of aquaporin-3 in the epidermis. *J. Invest. Dermatol.* 128, 2145–2151. doi: 10.1038/jid.2008.70
- Huang, Z., Zhong, C., Dai, J., Li, S., Zheng, M., He, Y., et al. (2021). Simultaneous enhancement on renewable bioactive compounds from *Porphyridium cruentum* via a novel two-stage cultivation. *Algal Res.* 55, 102270. doi: 10.1016/j.algal.2021.102270
- Isailovic, D., Sultana, I., Phillips, G. J., and Yeung, E. S. (2006). Formation of fluorescent proteins by the attachment of phycoerythrobilin to R-phycoerythrin alpha and beta apo-subunits. *Anal. Biochem.* 358, 38–50. doi: 10.1016/j.ab.2006.08.011
- Jaubert, M., Bouly, J.-P., d'Alcalá, M. R., and Falcioro, A. (2017). Light sensing and responses in marine microalgae. *Curr. Opin. Plant Biol.* 37, 70–77. doi: 10.1016/j.pbi.2017.03.005
- Jeon, M. S., Han, S.-I., Jeon, M., and Choi, Y.-E. (2021). Enhancement of phycoerythrin productivity in *Porphyridium purpureum* using the clustered regularly interspaced short palindromic repeats/CRISPR-associated protein 9 ribonucleoprotein system. *Bioresour. Technol.* 330, 124974. doi: 10.1016/j.biortech.2021.124974
- Kim, H., Lim, Y.-j., Park, J.-H., and Cho, Y. (2012). Dietary silk protein, sericin, improves epidermal hydration with increased levels of filaggrins and free amino acids in NC/Nga mice. *Br. J. Nutr.* 108, 1726–1735. doi: 10.1017/S0007114511007306
- Kwan, P. P., Banerjee, S., Shariff, M., and Md. Yusoff, F. (2021). Influence of light on biomass and lipid production in microalgae cultivation. *Aquac. Res.* 52, 1337–1347. doi: 10.1111/are.15023
- Lauceri, R., Zittelli, G. C., and Torzillo, G. (2019). A simple method for rapid purification of phycobiliproteins from *Arthrospira platensis* and *Porphyridium cruentum* biomass. *Algal Res.* 44, 101685. doi: 10.1016/j.algal.2019.101685
- Lee, C., Choi, Y.-E., and Yun, Y.-S. (2016). A strategy for promoting astaxanthin accumulation in *Haematococcus pluvialis* by 1-aminocyclopropane-1-carboxylic acid application. *J. Biotechnol.* 236, 120–127. doi: 10.1016/j.jbiotec.2016.08.012
- Lee, E., Jalalizadeh, M., and Zhang, Q. (2015). Growth kinetic models for microalgae cultivation: A review. *Algal Res.* 12, 497–512. doi: 10.1016/j.algal.2015.10.004
- Leney, A. C., Tschanz, A., and Heck, A. J. (2018). Connecting color with assembly in the fluorescent B-phycoerythrin protein complex. *FEBS J.* 285, 178–187. doi: 10.1111/febs.14331
- Li, S., Ji, L., Shi, Q., Wu, H., and Fan, J. (2019). Advances in the production of bioactive substances from marine unicellular microalgae *Porphyridium* spp. *Bioresour. Technol.* 292, 122048. doi: 10.1016/j.biortech.2019.122048
- Liberman, G. N., Ochbaum, G., Mejubovsky-Mikhelis, M., Bitton, R., and Arad, S. M. (2020). Physico-chemical characteristics of the sulfated polysaccharides of the red microalgae *Dixonella grisea* and *Porphyridium aeruginum*. *Int. J. Biol. Macromol.* 145, 1171–1179. doi: 10.1016/j.ijbiomac.2019.09.205
- Lin, G., Wang, Y., Guo, L., Ding, H., Hu, Y., Liang, S., et al. (2017). Verification of mutagen function of Zeocin in *Nannochloropsis oceanica* through transcriptome analysis. *J. Ocean Univ.* 16, 501–508. doi: 10.1007/s11802-017-3231-x
- Liu, Y., Feng, Y., and Lun, J. (2012). Aqueous two-phase countercurrent distribution for the separation of c-phycoerythrin and allophycocyanin from *Spirulina platensis*. *Food Bioprod. Process.* 90, 111–117. doi: 10.1016/j.fbp.2011.08.002
- Ma, Y., Xie, J., Zhang, R., Hu, C., and Zhao, J. (2008). Molecular properties of R-phycoerythrin subunits from *Polysiphonia urceolata* in potassium phosphate buffer. *Photochem. Photobiol. Sci.* 7, 263–268. doi: 10.1039/b714837b
- Munier, M., Jubeau, S., Wijaya, A., Morançais, M., Dumay, J., Marchal, L., et al. (2014). Physicochemical factors affecting the stability of two pigments: R-phycoerythrin of *Grateloupia turururu* and B-phycoerythrin of *Porphyridium cruentum*. *Food Chem.* 150, 400–407. doi: 10.1016/j.foodchem.2013.10.113
- Osorio, H., Jara, C., Fuenzalida, K., Rey-Jurado, E., and Vásquez, M. (2019). High-efficiency nuclear transformation of the microalgae *Nannochloropsis oceanica* using Tn5 Transposome for the generation of altered lipid accumulation phenotypes. *Biotechnol. Biofuels* 12, 1–12. doi: 10.1186/s13068-019-1475-y
- Ozsvar, J., Yang, C., Cain, S. A., Baldock, C., Tarakanova, A., and Weiss, A. S. (2021). Tropoelastin and elastin assembly. *Front. Bioeng. Biotechnol.* 9, 643110. doi: 10.3389/fbioe.2021.643110
- Park, S., Nguyen, T. H. T., and Jin, E. (2019). Improving lipid production by strain development in microalgae: strategies, challenges and perspectives. *Bioresour. Technol.* 292, 121953. doi: 10.1016/j.biortech.2019.121953
- Peña-Medina, R. L., Fimbres-Olivarria, D., Enriquez-Ocaña, L. F., Martínez-Córdova, L. R., Del-Toro-Sánchez, C. L., López-Elias, J. A., et al. (2023). Erythroprotective potential of phycobiliproteins extracted from *porphyridium cruentum*. *Metabolites* 13, 366. doi: 10.3390/metabo13030366
- Ramirez, F., and Sakai, L. Y. (2010). Biogenesis and function of fibrillin assemblies. *Cell Tissue Res.* 339, 71–82. doi: 10.1007/s00441-009-0822-x
- Risjani, Y., Mutmainnah, N., Manurung, P., and Wulan, S. N. (2021). Exopolysaccharide from *Porphyridium cruentum* (purpureum) is not toxic and stimulates immune response against vibriosis: the assessment using zebrafish and white shrimp *Litopenaeus vannamei*. *Mar. Drugs* 19, 133. doi: 10.3390/md19030133
- Romana-Souza, B., Silva-Xavier, W., and Monte-Alto-Costa, A. (2020). Topical application of a commercially available formulation of vitamin C stabilized by vitamin E and ferulic acid reduces tissue viability and protein synthesis in ex vivo human normal skin. *J. Cosmet. Dermatol.* 19, 2965–2973. doi: 10.1111/jocd.13413
- Schiano di Visconte, G., Spicer, A., Chuck, C. J., and Allen, M. J. (2019). The microalgae biorefinery: a perspective on the current status and future opportunities using genetic modification. *Appl. Sci.* 9, 4793. doi: 10.3390/app9224793
- Schulze, P. S., Barreira, L. A., Pereira, H. G., Perales, J. A., and Varela, J. C. (2014). Light emitting diodes (LEDs) applied to microalgal production. *Trends Biotechnol.* 32, 422–430. doi: 10.1016/j.tibtech.2014.06.001
- Sepúlveda-Ugarte, J., Brunet, J. E., Matamala, A. R., Martínez-Oyanedel, J., and Bunster, M. (2011). Spectroscopic parameters of phycoerythrobilin and phycourobilin on phycoerythrin from *Gracilaria Chilensis*. *J. Photochem. Photobiol. A-Chem.* 219, 211–216. doi: 10.1016/j.jphotochem.2011.02.012
- Sirisuk, P., Ra, C.-H., Jeong, G.-T., and Kim, S.-K. (2018). Effects of wavelength mixing ratio and photoperiod on microalgal biomass and lipid production in a two-phase culture system using LED illumination. *Bioresour. Technol.* 253, 175–181. doi: 10.1016/j.biortech.2018.01.020
- Sonani, R., Rastogi, R., and Madamwar, D. (2015). Antioxidant potential of phycobiliproteins: Role in anti-aging research. *Biochem. Anal. Biochem.* 4, 2161–1009. doi: 10.4172/2161-1009
- Srinuanpan, S., Cheirsilp, B., and Prasertsan, P. (2018). Effective biogas upgrading and production of biodiesel feedstocks by strategic cultivation of oleaginous microalgae. *Energy* 148, 766–774. doi: 10.1016/j.energy.2018.02.010

- Sun, L., Wang, C., Shi, Q., and Ma, C. (2009). Preparation of different molecular weight polysaccharides from *Porphyridium cruentum* and their antioxidant activities. *Int. J. Biol. Macromol.* 45, 42–47. doi: 10.1016/j.ijbiomac.2009.03.013
- Tang, D. Q., Zou, L., Yin, X. X., and Ong, C. N. (2016). HILIC-MS for metabolomics: An attractive and complementary approach to RPLC-MS. *Mass Spectrom. Rev.* 35, 574–600. doi: 10.1002/mas.21445
- Tharakan, S., Pontiggia, L., Biedermann, T., Böttcher-Haberzeth, S., Schiestl, C., Reichmann, E., et al. (2010). Transglutaminases, involucrin, and loricrin as markers of epidermal differentiation in skin substitutes derived from human sweat gland cells. *Pediatr. Surg. Int.* 26, 71–77. doi: 10.1007/s00383-009-2517-5
- Thomson, J., Singh, M., Eckersley, A., Cain, S. A., Sherratt, M. J., and Baldock, C. (2019). Fibrillin microfibrils and elastic fibre proteins: functional interactions and extracellular regulation of growth factors. *Semi. Cell Dev. Biol.* 89, 109–117. doi: 10.1016/j.semcdb.2018.07.016
- Thurakit, T., Pathom-Aree, W., Pumas, C., Brocklehurst, T. W., Pekkoh, J., and Srinuanpan, S. (2022). High-efficiency production of biomass and biofuel under two-stage cultivation of a stable microalga *Botryococcus braunii* mutant generated by ethyl methanesulfonate-induced mutation. *Renew. Energy* 198, 176–188. doi: 10.1016/j.renene.2022.08.029
- Trovão, M., Schüler, L. M., MaChado, A., Bombo, G., Navalho, S., Barros, A., et al. (2022). Random mutagenesis as a promising tool for microalgal strain improvement towards industrial production. *Mar. Drugs* 20, 440. doi: 10.3390/md20070440
- Tsukui, K., Kakiuchi, T., Suzuki, M., Sakurai, H., and Tokudome, Y. (2022). The ion balance of Shotokuseki extract promotes filaggrin fragmentation and increases amino acid production and pyrrolidone carboxylic acid content in three-dimensional cultured human epidermis. *Nat. Product. Bioprospecting* 12, 37. doi: 10.1007/s13659-022-00353-0
- Watanabe, M., and Ikeuchi, M. (2013). Phycobilisome: architecture of a light-harvesting supercomplex. *Photosynth. Res.* 116, 265–276. doi: 10.1007/s11120-013-9905-3
- Yokono, M., Murakami, A., and Akimoto, S. (2011). Excitation energy transfer between photosystem II and photosystem I in red algae: larger amounts of phycobilisome enhance spillover. *Biochim. Biophys. Acta-Bioenerg.* 1807, 847–853. doi: 10.1016/j.bbabi.2011.03.014